Applied Energy 295 (2021) 117034

Contents lists available at ScienceDirect

Applied Energy

journal homepage: www.elsevier.com/locate/apenergy

New data optimization framework for parameter estimation under uncertainties with application to lithium-ion battery

Qingzhi Lai [a], Hyoung Jun Ahn [b], YoungJin Kim [b], You Na Kim [b], Xinfan Lin [a,*]

[a] Department of Mechanical and Aerospace Engineering, University of California, Davis, CA 95616, USA
[b] LG Energy Solution, Seoul, Republic of Korea

ARTICLE INFO

Keywords:
Estimation
Uncertainty
Data analysis
Data optimization
Sensitivity
Lithium-ion battery

ABSTRACT

Data optimization, or optimal experiment design, is an effective way to improve and guarantee the accuracy of state and parameter estimation, as the quality of data has significant impact on the estimation accuracy. Such capability is especially critical for energy systems requiring high reliability. The common practice of data optimization is to design input excitation by maximizing the Fisher information, and hence minimizes the variance of the estimation error. However, such approach suffers from fundamental limitations, including negligence of estimation bias and system uncertainties in measurement, model, and parameter, which severely restrict the applicability and effectiveness of the method. This paper aims at establishing new criteria and a novel framework for data optimization and estimation error quantification to overcome the fundamental limitations. First, a generic formula is derived for quantifying the estimation error subject to sensor, model, and parameter uncertainties for the commonly used least-squares algorithm. Based on the formula, desirable data structures, which could minimize the errors caused by each uncertainty, are identified. These structures are then used as new criteria to formulate the novel data optimization framework. The proposed methodology is applied to the parameter estimation problem of a lithium-ion battery electrochemical model in simulation and experiments, showing up to two orders of magnitude improvement in estimation accuracy compared with the traditional Fisher-information-based approach and other baselines.

1. Introduction

Parameter estimation is an important topic in modeling and control research, as the accuracy of estimation determines the fidelity of the model, and hence the performance of the commonly applied model-based estimation, diagnostics, and control. Due to its importance, estimation is a ubiquitous topic in different energy system applications, including batteries [1–3], renewable energy generation systems [4,5], and power distribution systems [6,7] among others. The process of estimation typically involves 3 basic elements, i.e. model, algorithm, and data, as the algorithm fits the data to the model to generate the best estimates of the parameters.

As it has been recognized that the quality of data plays an important role in determining the accuracy of the estimation results, research on data analysis and optimization has been receiving increasing attention recently. Take the field of battery control research as an example. On one hand, researchers have been studying the relationship between estimation accuracy and data, with relevant topics including error quantification [8–10], sensitivity analysis [11–13], and Fisher information (FI) and Cramér–Rao bound derivation for battery equivalent-circuit models [14–16] and the Doyle–Fuller–Newman model [17] among others. This theme of research started with simplified macroscopic battery models, e.g. coulomb counting and equivalent circuit models, and has recently delved into analytical analysis for complicated first-principle electrochemical models [18,19]. On the other hand, optimization of data to improve the estimation accuracy has also attracted significant attention. The goal is to answer a fundamental question, i.e. what is the input excitation sequence that could generate the optimal response data for estimating a certain or a group of model parameters? The common practice is to design input excitation to maximize the information content (e.g. sensitivity-based Fisher information) of the response data about the target variable for estimation [20,21]. Due to the complexity of sensitivity and Fisher information computation, especially for the electrochemical battery models, most works imposed certain patterns on the input excitation, e.g. sinusoidal or pulse [20–22], to facilitate the optimization process. Recently, major progress has been made to find the ultimate optimal input with no imposed pattern [23], based on analytically derived and simplified sensitivity computation techniques [19].

* Corresponding author.
E-mail address: lxflin@ucdavis.edu (X. Lin).

https://doi.org/10.1016/j.apenergy.2021.117034
Received 25 February 2021; Received in revised form 23 April 2021; Accepted 27 April 2021
Available online 7 May 2021
0306-2619/© 2021 Elsevier Ltd. All rights reserved.

Despite encouraging progress and promising outlook, there are major limitations with the existing methodology and practice of data optimization for estimation. Specifically, the "gold standard" has been the Fisher information [24], which is the most widely used metric for evaluating and optimizing the quality of data. However, such metric suffers from several fundamental deficiencies. First, Fisher information is theoretically only related to the variance of estimation error under the assumption of no estimation bias. By inverting the Fisher information, the Cramér–Rao bound of the estimate can be obtained, which indicates the best achievable variance of the estimation error for an unbiased estimator [24]. This is a highly restrictive assumption as in practice estimation bias is not only inevitable, but also often more critical than variance [9]. Second, the Fisher information (FI)/Cramér–Rao bound-based approach only looks to minimize the error variance caused by measurement variance, but neglects other types of commonly presented constant and varying uncertainties in measurement, model, and parameter. In fact, there is not even a systematic way to quantify the estimation error under these uncertainties, let alone reduce/eradicate the error. In addition, the Cramér–Rao bound only gives the best achievable variance in theory with no guarantee that it can be attained in practice (especially for nonlinear systems). All these limitations severely undermine the effectiveness of the conventional data optimization approach, and hence the obtained optimal input profile often only achieves minimal or even no improvement in the estimation results.

The objective of this work is to overcome the fundamental limitations of the conventional approach by establishing new criteria and framework for estimation error quantification and data optimization. We first derive a formula to quantify the estimation error caused by measurement, model, and parameter uncertainties for the least-squares algorithm, which is the most commonly used method for parameter estimation. It is interesting to find that Fisher information is only part of the equation, and there are other desirable data structures related to sensitivity that would contribute to error reduction. Based on these findings, we define new criteria and problem formulations to perform data optimization for improving estimation accuracy. Solving the new problems requires fast and efficient computation and optimization of parameter sensitivity, which is enabled by analytical sensitivity computation techniques [18,19]. The new framework has been applied to parameter estimation of a lithium-ion battery electrochemical model in simulation and experiments, showing up to two orders-of-magnitude improvement in accuracy compared with the traditional FI-based approach and other baselines.

2. Derivation of new formula for quantifying estimation error under uncertainties

In this section, we derive a formula which quantifies the parameter estimation error for the least-squares method. To the best of our knowledge, this formula is the first one capable of systematically predicting the estimation errors caused by uncertainties in measurement, model, and parameters, which enables the identification of desirable data structures for improving estimation accuracy. Consider a generic discrete-time dynamic system described by

$$\begin{aligned} x_k &= f_k(x_{k-1}, \boldsymbol{\theta}, u_{k-1}) \\ y_k &= g_k(x_k, \boldsymbol{\theta}, u_k), \end{aligned} \tag{1}$$

where subscript k denotes the discrete time instant, $\boldsymbol{\theta} = [\theta_1, \theta_2, \dots, \theta_n]$ are the constant model parameters, u is the input, x are the states, and y is the output. Here we consider single-input-single-output systems with scalar u and y, but the analysis can be generalized to multi-input and output systems. Suppose we want to estimate one parameter θ_1 based on a sequence of N input data and the resultant output data

$$\boldsymbol{y^m} = [y_1^m, y_2^m, \dots, y_N^m], \tag{2}$$

where y^m denotes the measured output value,

$$y_k^m = y_k(\boldsymbol{\theta}) + \Delta y + \delta y_k. \tag{3}$$

In Eq. (3), $y_k(\boldsymbol{\theta})$ represents the output predicted by the model in Eq. (1) based on the true parameter $\boldsymbol{\theta}$, Δy stands for the constant mismatch between y_k and the true system output including both model and measurement bias, and δy_k denotes the varying uncertainty in model and measurement. The least-squares estimation problem is then formulated as

$$\min_{\hat{\theta}_1} J = \frac{1}{2}\sum_{k=1}^{N}\left(y_k^m(\boldsymbol{\theta}) - \hat{y}_k(\hat{\boldsymbol{\theta}})\right)^2, \tag{4}$$

where $\hat{y}_k(\hat{\boldsymbol{\theta}})$ is the model output based on the estimated/assumed parameter value $\hat{\boldsymbol{\theta}}$,

$$\hat{\boldsymbol{\theta}} = \left[\hat{\theta}_1, \hat{\theta}_2, \dots, \hat{\theta}_n\right]. \tag{5}$$

It is noted that $\hat{\theta}_1$ is the target variable for estimation by solving Eq. (4), while $\hat{\theta}_2, \dots, \hat{\theta}_n$ represent the assumed values for other parameters with uncertainty.

The estimate $\hat{\theta}_1$ can be found based on the first-order optimality condition $\frac{\partial J}{\partial \hat{\theta}_1} = 0$, as

$$\sum_{k=1}^{N}\left(y_k^m - \hat{y}_k\right)\frac{\partial\left(y_k^m - \hat{y}_k\right)}{\partial \hat{\theta}_1} = 0, \tag{6}$$

with

$$y_k^m - \hat{y}_k = y_k(\boldsymbol{\theta}) + \Delta y + \delta y_k - y_k(\hat{\boldsymbol{\theta}}). \tag{7}$$

By taking the first-order Taylor expansion about $\hat{\boldsymbol{\theta}}$, Eq. (7) can be expanded as

$$\begin{aligned} y_k^m - \hat{y}_k &\approx \frac{\partial y_k}{\partial \boldsymbol{\theta}}(\hat{\boldsymbol{\theta}})\Delta\boldsymbol{\theta} + \Delta y + \delta y_k \\ &= \frac{\partial y_k}{\partial \theta_1}(\hat{\boldsymbol{\theta}})\Delta\theta_1 + \cdots + \frac{\partial y_k}{\partial \theta_n}(\hat{\boldsymbol{\theta}})\Delta\theta_n + \Delta y + \delta y_k \end{aligned} \tag{8}$$

where $\Delta\theta_1 = \theta_1 - \hat{\theta}_1$ represents the estimation error in θ_1, $\Delta\theta_2 = \theta_2 - \hat{\theta}_2, \dots$, $\Delta\theta_n = \theta_n - \hat{\theta}_n$ denote the mismatch/uncertainty in other parameters, and $\frac{\partial y_k}{\partial \theta_i}(\hat{\boldsymbol{\theta}})$ is the output sensitivity of parameter θ_i (evaluated at $\hat{\boldsymbol{\theta}}$). To minimize the error introduced by the first-order Taylor expansion, a reasonable initial guess of parameter values can be obtained by adopting nominal values in relevant literature for a battery with similar chemistry. The results shown in our prior work [25] and Sections 4 and 5 of this paper demonstrate the robustness of our data optimization approach to such deviation in initial guess. Meanwhile, it is also possible to establish the error bounds on the result by exploring higher order derivatives. By taking the partial derivative of Eq. (7) to θ_1, we have

$$\frac{\partial\left(y_k^m - \hat{y}_k\right)}{\partial \hat{\theta}_1} = -\frac{\partial \hat{y}_k}{\partial \hat{\theta}_1} = -\frac{\partial y_k}{\partial \theta_1}(\hat{\boldsymbol{\theta}}). \tag{9}$$

Finally, by substituting Eqs. (8) and (9) into (6) and reformulating, an expression for the estimation error $\Delta\theta_1$ can be obtained as Eq. (10) given in Box I. Eq. (10) quantifies the error induced by constant model/measurement uncertainty Δy_k, varying model/measurement uncertainty δy_k, and uncertainty in other parameters $\Delta\theta_2, \dots, \Delta\theta_n$.

Several important insights on estimation errors can be made from Eq. (10) as follows.

1. The denominator, $\sum_{k=1}^{N}\left(\frac{\partial y_k}{\partial \theta_1}\right)^2$, is essentially the Fisher information of the target variable θ_1 (simplified under i.i.d. Gaussian noise) [26,27], which has been the predominantly used objective for data optimization [21,23]. Eq. (10) establishes the direct link between Fisher information and estimation error, and is more intuitive and applicable than the restrictive Cramér–Rao Bound interpretation. It is interesting to note that, on one hand,

$$\Delta\theta_1 = -\frac{\left(\sum_{k=1}^{N}\frac{\partial y_k}{\partial\theta_1}(\hat{\theta})\right)\Delta y + \left(\sum_{k=1}^{N}\frac{\partial y_k}{\partial\theta_1}(\hat{\theta})\delta y_k\right) + \left(\sum_{k=1}^{N}\frac{\partial y_k}{\partial\theta_2}(\hat{\theta})\frac{\partial y_k}{\partial\theta_1}(\hat{\theta})\right)\Delta\theta_2 + \cdots + \left(\sum_{k=1}^{N}\frac{\partial y_k}{\partial\theta_n}(\hat{\theta})\frac{\partial y_k}{\partial\theta_1}(\hat{\theta})\right)\Delta\theta_n}{\sum_{k=1}^{N}\left(\frac{\partial y_k}{\partial\theta_1}(\hat{\theta})\right)^2} \tag{10}$$

Box I.

maximizing Fisher information could indeed reduce the estimation error by increasing the denominator; on the other, Fisher information is only part of the formula as the numerator terms also have major impacts.

2. The first term in the numerator, $\left(\sum_k^N \frac{\partial y_k}{\partial\theta_1}\right)\Delta y$, represents the estimation error caused by constant model/measurement uncertainty Δy. It shows that such error can be eradicated by making $\sum_k^N \frac{\partial y_k}{\partial\theta_1} = 0$, i.e. zero sum of sensitivity of θ_1 over the whole data sequence. This finding indicates the fundamental data structure for improving estimation accuracy under constant model/measurement bias, which has not been established in literature before. It is noted that there is a tradeoff between minimizing this term and maximizing the Fisher information (sensitivity magnitude), and both need to be considered in order to attain the best estimation accuracy. The new data optimization framework to be demonstrated in Section 3 is formulated by exploiting such tradeoff. Similar tradeoffs also apply to terms associated with other types of uncertainties to be discussed subsequently.
3. The second term in the numerator, $\sum_k^N \frac{\partial y_k}{\partial\theta_1}\delta y_k$, represents the estimation error caused by varying model/measurement uncertainty δy_k. This term is essentially the inner product of the sensitivity sequence vector $\frac{\partial \mathbf{y}}{\partial\theta_1} = [\frac{\partial y_1}{\partial\theta_1}, \frac{\partial y_2}{\partial\theta_1}, \ldots, \frac{\partial y_N}{\partial\theta_1}]^T$ with the uncertainty sequence vector $\delta\mathbf{y} = [\delta y_1, \delta y_2, \ldots, \delta y_N]^T$. It shows that the error can be eradicated by having $\sum_k^N \frac{\partial y_k}{\partial\theta_1}\delta y_k = 0$ or $\frac{\partial \mathbf{y}}{\partial\theta_1}\cdot\delta\mathbf{y} = 0$, i.e. making the sensitivity vector orthogonal to the uncertainty vector. This finding indicates the data structure for improving estimation accuracy under varying model/measurement uncertainty, which is also unexplored in literature.
4. The remaining terms in the numerator, $\left(\sum_k^N \frac{\partial y_k}{\partial\theta_i}\frac{\partial y_k}{\partial\theta_1}\right)\Delta\theta_i$, reflect the error caused by uncertainty in other parameters. The terms are essentially the inner product of the sensitivity vector of the target variable θ_1 with that of uncertain parameter θ_i times the amount of uncertainty $\Delta\theta_i$. The error can be eradicated by having $\sum_k^N \frac{\partial y_k}{\partial\theta_1}\frac{\partial y_k}{\partial\theta_i} = 0$ or $\frac{\partial \mathbf{y}}{\partial\theta_1}\cdot\frac{\partial \mathbf{y}}{\partial\theta_i} = 0$, i.e. making the sensitivity vector of the target parameter orthogonal to those of uncertain parameters. This finding is related to our prior results on multivariate Cramér–Rao bound analysis [27], which showed that data with orthogonal parameter sensitivity could reduce the error variance for joint estimation of two parameters. This data structure is also a new one to be incorporated into data optimization.

The developed methodology in this paper is applicable to multi-input-multi-output (MIMO) systems, in which the parameter sensitivity is driven by multiple inputs while different outputs will have different sensitivity dynamics. Specifically, for multiple-input (MI) systems, the data structures for rejecting uncertainties are the same, except that the sensitivity expression will be more complicated containing multiple terms with respect to different inputs. Therefore, the data optimization procedures will need to optimize multiple input sequences, resulting in a more complicated problem to solve. For multiple-output (MO) systems, the data structures for rejecting uncertainties need to be re-derived by re-formulating the least-squares cost function to incorporate multiple outputs and applying the first-order optimality condition.

3. New data optimization framework

In this section, we propose a new data optimization (or optimal experiment design) framework for parameter estimation with the goal of minimizing the errors caused by uncertainties in measurement, model, and parameters, based on the desirable data structures extracted from Eq. (10). The framework is built upon new problem formulations and efficient parameter sensitivity computation techniques.

3.1. New criteria and problem formulation

Traditionally, data optimization (or optimal experiment design) for parameter estimation is performed by maximizing the Fisher information [21,23]. For single parameter estimation, the problem takes the form (assuming i.i.d. Gaussian noise),

$$\underset{\boldsymbol{u}}{Max}\sum_{k=1}^{N}\left(\frac{\partial y_k}{\partial\theta_1}(\boldsymbol{u},\hat{\theta})\right)^2, \tag{11}$$

where the decision variables are the control input sequence $\boldsymbol{u} = [u_1, u_2, \ldots, u_N]^T$ which could change the sensitivity level through the system dynamics. It is noted that $\frac{\partial y_k}{\partial\theta_1}(\boldsymbol{u},\hat{\theta})$ denotes the sensitivity of θ_1 evaluated at certain *a priori* parameter values $\hat{\theta}$, because sensitivity is parameter value dependent, and the exact parameter values are unknown for data optimization. As discussed previously, maximizing Fisher information could indeed reduce the error according to Eq. (10), but this alone will not necessarily minimize the error as there are other desirable data structures that would contribute to error reduction as identified from the numerator of Eq. (10).

In the case with constant model/measurement bias Δy, a new optimization problem can be formulated as

$$\underset{\boldsymbol{u}}{Max}\sum_{k=1}^{N}\left(\frac{\partial y_k}{\partial\theta_1}(\boldsymbol{u},\hat{\theta})\right)^2 - \alpha\left|\sum_{k=1}^{N}\frac{\partial y_k}{\partial\theta_1}(\boldsymbol{u},\hat{\theta})\right|, \tag{12}$$

which, besides maximizing the Fisher information, adds a soft constraint to minimize $\left|\sum_k^N \frac{\partial y_k}{\partial\theta_1}(\boldsymbol{u},\hat{\theta})\right|$ through a weight factor α. The new formulation is based on the previous analysis on Eq. (10), which discovers that making $\sum_k^N \frac{\partial y_k}{\partial\theta_1} = 0$ could eradicate the estimation error caused by constant bias Δy. The problem can also be formulated as maximizing Fisher information subject to a hard constraint on $\sum_k^N \frac{\partial y_k}{\partial\theta_1} = 0$. Constant or slow-varying model/measurement bias is a common source of estimation error in practice [10], which can be caused by sensor/model drift due to change in operating condition or degradation. We will show with an example later that the new approach could enable far superior estimation accuracy than the Fisher-information only approach.

In the case of parameter uncertainty, e.g. in one parameter θ_2, a new optimization problem can be formulated as

$$\underset{\boldsymbol{u}}{Max}\sum_{k=1}^{N}\left(\frac{\partial y_k}{\partial\theta_1}(\boldsymbol{u},\hat{\theta})\right)^2 - \alpha\left|\sum_{k=1}^{N}\frac{\partial y_k}{\partial\theta_1}(\boldsymbol{u},\hat{\theta})\frac{\partial y_k}{\partial\theta_2}(\boldsymbol{u},\hat{\theta})\right|, \tag{13}$$

by adding a soft constraint to minimize $\left|\sum_k^N \frac{\partial y}{\partial\theta_1}(\boldsymbol{u},\hat{\theta})\frac{\partial y}{\partial\theta_2}(\boldsymbol{u},\hat{\theta})\right|$. This new formulation is based on the previous discovery that making $\sum_k^N \frac{\partial y}{\partial\theta_1}\frac{\partial y}{\partial\theta_2} = 0$ could eradicate the estimation error caused by $\Delta\theta_2$. Eq. (13) can be augmented with more terms to accommodate uncertainty in more parameters. Parameter uncertainty is usually inevitable

in practice [8]. On one hand, for systems with a large number of parameters, the identification procedure is typically sequential with some parameters being estimated first without knowing others [21]. On the other, it is often only of interest to estimate a subset of parameters. We will show that the new formulation could yield far superior results than the FI-based approach in such scenario.

Similarly, in the case of varying measurement/model uncertainty δy_k, a new problem can be formulated by adding $\sum_k^N \frac{\partial y_k}{\partial \theta_1}\delta y_k = 0$ as either a hard or soft constraint. This new problem formulation is also of significant practical interest due to the inevitable model uncertainty. On one hand, no model is capable of capturing the dynamics of a system perfectly, no matter how complicated the model is. On the other, common model simplification techniques to facilitate control applications, e.g. model reduction [28] and linearization, introduce extra uncertainty. The new formulation indicates a way to address model uncertainty by considering it as an additive part of the model output. Specifically, if the dynamics/model of varying model/measurement uncertainty δy_k can be captured in whole or in part, for example in [29], it is possible then to design a profile that can mitigate the impact of δy_k by leveraging the sensitivity orthogonality. On the other hand, if there is completely no knowledge of δy_k, model-free methods for design can be exploited, e.g. reinforcement learning, which does not need to explicitly know/predict the dynamics of uncertainty, but rather explore and learn through interactive experiments with the real battery. Furthermore, it is possible to use the proposed data optimization approach for estimating the model uncertainty δy_k itself as well. For example, if the uncertainty can be characterized by a model with certain unknown parameters, the method can be used to design optimal input excitation for parameterizing the uncertainty model.

Finally, for the general case of estimation subject to uncertainties in measurement, multi-parameters, and model, the data optimization problem is formulated as in Eq. (14) by combining all previous cases.

$$\begin{aligned}\max_{\boldsymbol{u}} \sum_{k=1}^{N}\left(\frac{\partial y_k}{\partial \theta_1}(\boldsymbol{u},\hat{\theta})\right)^2 &- \alpha_1\left|\sum_{k=1}^{N}\frac{\partial y_k}{\partial \theta_2}(\boldsymbol{u},\hat{\theta})\frac{\partial y_k}{\partial \theta_1}(\boldsymbol{u},\hat{\theta})\right| \cdots \\ &- \alpha_{n-1}\left|\sum_{k=1}^{N}\frac{\partial y_k}{\partial \theta_n}(\boldsymbol{u},\hat{\theta})\frac{\partial y_k}{\partial \theta_1}(\boldsymbol{u},\hat{\theta})\right| \\ &- \alpha_n\left|\sum_{k=1}^{N}\frac{\partial y_k}{\partial \theta_1}(\boldsymbol{u},\hat{\theta})\right| - \alpha_{n+1}\left|\sum_{k=1}^{N}\frac{\partial y_k}{\partial \theta_1}(\boldsymbol{u},\hat{\theta})\delta y_k\right|\end{aligned} \tag{14}$$

The factors $\alpha_1, \ldots, \alpha_{n+1}$ are the weights for penalizing different uncertainty sources, and their values can be tuned based on estimates of the magnitude of respective uncertainties.

It is noted that the current problem formulation is for single-variate estimation, but can be easily extended to the multivariate case. In the latter case, a commonly used metric for data optimization is the determinant of the Fisher information matrix [20,21,30], which is the Fisher info itself in the single-variate case. The derivation for the multivariate case is underway, and it is speculated that the determinant of Fisher information will appear in the denominator of the equivalent error formula, indicating one data structure for optimizing the accuracy. Meanwhile, similar to the single-variate case, there will be terms in the numerator indicating other data structures associated with uncertainties. These data structures will be utilized to formulate the data optimization framework for multivariate estimation.

3.2. Computation of parameter sensitivity

One key to solve the formulated new optimization problems is the sensitivity computation for the target variable under estimation $\frac{\partial y_k}{\partial \theta_1}(\boldsymbol{u},\hat{\theta})$ and other uncertain parameters $\frac{\partial y_k}{\partial \theta_i}(\boldsymbol{u},\hat{\theta})$. Traditional methods for sensitivity computation include manual perturbation [11,13] or solving the sensitivity differential equation (SDE) [31], which are highly computationally intensive and often intractable for data optimization, especially for systems of high or infinite dimension, e.g. PDEs [21].

We have formulated a methodology to derive analytic expressions for parameter sensitivity of semi-linear ODE and PDE-based systems [15,19] to enable efficient sensitivity computation. Specifically, it is found that the parameter sensitivity generally consists of a (linear) dynamic term, which reflects the impact of the parameter on the output through a dynamic process, e.g. diffusion, and non-dynamic terms, which reflect the instantaneous effects, e.g. Ohm's law. The dynamic term causes the major difficulty for computation. By leveraging model reformulation and reduction techniques including Laplace transform and Padé approximation, we managed to derive a compact analytic expression for the dynamic sensitivity in the form of a sensitivity transfer function (STF).

As an example for illustration, in the context of a battery electrochemical (single particle) model, the sensitivity of the electrode lithium diffusion coefficient D_s takes the form

$$\frac{\partial V}{\partial D_s}(t) = \left(\frac{\partial \eta}{\partial c_{se}} + \frac{\partial U}{\partial c_{se}}\right)\cdot\frac{\partial c_{se}}{\partial D_s}(t), \tag{15}$$

where $\frac{\partial U}{\partial c_{se}}$ and $\frac{\partial \eta}{\partial c_{se}}$ are the slopes of the electrode open-circuit potential (OCP) and overpotential respectively, and $\frac{\partial c_{se}}{\partial D_s}$ is the sensitivity of the diffusion state, i.e. particle surface concentration c_{se}, to D_s. By applying the aforementioned methodology, an STF has been derived to characterize the dynamic nature of $\frac{\partial c_{se}}{\partial D_s}$,

$$\frac{\partial C_{se}}{\partial D_s}(s) = \frac{43R_s^4s^2 + 1980D_sR_s^2s + 38115D_s^2}{\left(R_s^4s^2 + 189D_sR_s^2s + 3465D_s^2\right)^2}\cdot\frac{21R_s^2}{F\varepsilon_s A\delta}I(s), \tag{16}$$

where R_s is the particle radius, F is the Faraday constant, A is the electrode area, δ is the electrode thickness, and ε_s is the active material volume fraction. The STF can be easily implemented in the time domain, e.g. through state space representation, for sensitivity computation or optimization. More details regarding the methodology and derived sensitivities for other battery electrochemical parameters can be found in [19].

4. Simulation verification with battery electrochemical model

In this section, we demonstrate the application of the data optimization framework to estimation of battery electrochemical parameters. We will compare the estimation results using the optimized input current profile with those using pulses [32,33], constant current [34,35], and dynamic drive cycle profiles [36], which are the heuristic profiles widely adopted in the practice of battery parameter estimation. Meanwhile, we will also compare with the profile optimized using the FI-based approach, which is the traditional method for optimal input/experiment design [16,21]. In this section, the studies will be performed in simulation using a single particle battery model with electrolyte dynamics (SPMe) [19], with the parameters adopted from [37] for an LGM50 INR21700 battery. The target variables for estimation are the electrode (cathode) active material volume fraction ε_s, and lithium diffusion coefficient D_s, which are critical parameters related to key battery performance [38,39]. We will present the results under different types of uncertainties, namely constant measurement/model bias and/or parameter uncertainty.

4.1. Estimation of active material volume fraction ε_s

4.1.1. Estimating ε_s under constant model/sensor bias

The first case of demonstration is estimating ε_s subject to constant model/measurement bias. In this case, the optimal current profile is obtained by solving Eq. (12) with $\theta_1 = \varepsilon_s$ and $\alpha = 1$, and the results are shown in Fig. 1. The initial SOC of the battery is set to 50% during optimization. For comparison, the profile optimized using the

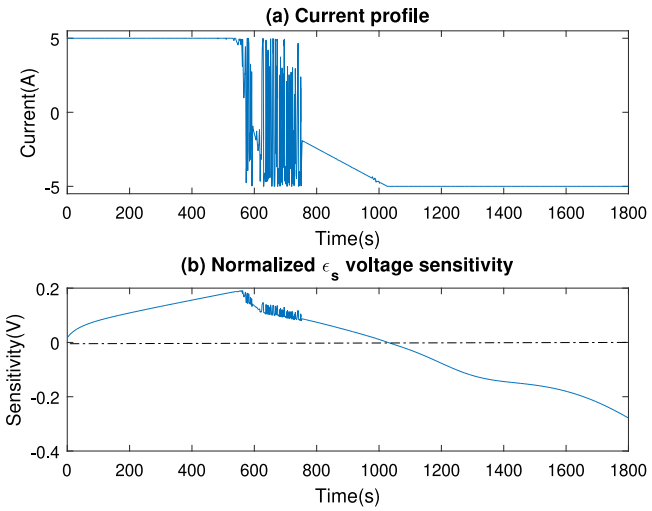

Fig. 1. Optimized current profile for estimating ϵ_s subject to constant voltage bias using new approach.

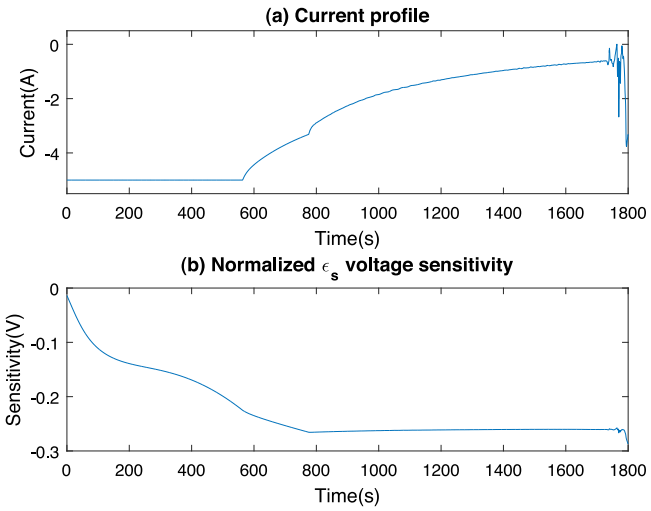

Fig. 2. Optimized current profile for estimating ϵ_s using FI-based approach.

traditional FI-based approach by solving Eq. (11) is also generated and shown in Fig. 2, of which the patterns have been explored in our prior work [23]. Both optimizations are performed assuming an *a priori* ϵ_s value that is 10% off the true value of 0.562, and subject to current constraint between −1C and +1C. It is noted that 10% deviation in ϵ_s translates to the same amount of mismatch in battery capacity, which is significant uncertainty as the battery is only supposed to lose 20% capacity over its lifetime according to the electric vehicle standard. Heuristic profiles commonly used for estimation in literature are also used for comparison, including constant current (CC) discharging at 1C, a pulse profile (with alternating 25 s 1C charge and discharge), and a dynamic drive cycle, i.e. Federal Urban Driving Schedule (FUDS). All profiles are of the same length (30 min) and number of data points (6000) to ensure fair comparison. For data generation, each current profile is fed to the SPMe model to obtain the response voltage data, which are then injected with a constant bias of −0.03 V to emulate the measurement/model bias. Same current profiles will be used for experimental validation in Section 5.

The estimation results using different profiles are summarized in Table 1. The table shows that the optimal current profile obtained based on the new approach gives the best accuracy, as it achieves the minimum estimation error at 0.089%, while the error of the traditional FI-based approach is at −11.9%, which is 133 times as large. Such dramatic difference can be explained by the evolution of sensitivity $\frac{\partial y_k}{\partial \epsilon_s}$ under the two profiles shown in Figs. 1(b) and 2(b) respectively. Specifically, under the profile obtained based on the new approach, $\frac{\partial y_k}{\partial \epsilon_s}$ distributes nearly equally above and below 0, giving a small (normalized) $\sum_k^N \frac{\partial y_k}{\partial \epsilon_s} = -3.67$, while the sensitivity under the profile of the FI-based approach is mostly negative, giving a (normalized) $\sum_k^N \frac{\partial y_k}{\partial \epsilon_s} = -1340$. Therefore, although the sensitivity of the latter is more prominent, giving higher (Fisher) information level, the profile does not yield good accuracy when subject to uncertainty. Moreover, Table 1 also validates Eq. (10) for error quantification, as the predicted estimation errors match well with the actual errors in general.

4.1.2. Estimating ϵ_s under bias and parameter uncertainty

In this case, we show the estimation of ϵ_s subject to both constant bias Δy and uncertainty in another battery parameter $\Delta\theta_2$, i.e. D_s. Data optimization using the new approach is performed by solving Eq. (14) with $\theta_1 = \epsilon_s$, $\theta_2 = D_s$, $\alpha_1 = 1$, $\alpha_n = 0.03$, and all other $\alpha = 0$. The optimal profiles obtained based on the new and FI-based approaches, along with other heuristic current profiles, are then used to generate the voltage output data in simulation. A constant −0.03 V bias is then injected to the voltage data to emulate the output bias, and during the process of estimating ϵ_s, the assumed value for D_s was deviated by 20% from the true value (used in simulation for data generation) to emulate the parameter uncertainty. The estimation results using different profiles are presented in Table 2, which shows that the profile designed by the new approach substantially outperforms all others. Specifically, the heuristic profiles, i.e. CC, pulse and dynamic cycle, all yield significant estimation errors above 10%, while the FI-based approach achieves major improvement by reducing the error to around −7%. Still, our new approach manages to yield a much smaller error at 1.44%, which is considered as highly accurate given the 20% uncertainty in D_s and the prominent constant voltage bias. The proposed approach achieves superior estimation accuracy by accommodating all 3 terms that contribute to the error during the multi-objective optimization procedures in this scenario, i.e. Fisher info, $\sum_k^N \frac{\partial y_k}{\partial \epsilon_s}\Delta y$ and $\sum_k^N \frac{\partial y_k}{\partial D_s}\frac{\partial y_k}{\partial \epsilon_s}\Delta\epsilon_s$. As shown in the last 3 columns of Table 2, the new approach does not manage to optimize any individual term, but instead achieves the optimal balance among them to minimize the error.

Table 1
Estimation results of ϵ_s under constant bias in simulation.

Profile	Actual error	Predicted error	FI	$\sum_{k=1}^N \frac{\partial y_k}{\partial \epsilon_s}$
New approach	0.0890%	−0.130%	83.8	−3.67
FI optimal	−11.9%	−14.0%	321	−1340
Pulse	19.1%	13.5%	3.38	18.7
1C CC	8.03%	7.59%	702	1930
FUDS	24.8%	18.6%	74.2	613

Table 2
Estimation results of ϵ_s under constant bias and parameter uncertainty in simulation.

Profile	Actual error	Predicted error	FI	$\sum \frac{\partial y_k}{\partial \epsilon_s}$	$\sum \frac{\partial y_k}{\partial D_s}\cdot\frac{\partial y_k}{\partial \epsilon_s}$
New approach	1.44%	0.46%	58.4	−128	24.8
FI optimal	−6.93%	−8.93%	369	−1430	72.3
Pulse	17.2%	12.9%	3.29	17.8	−0.127
1C CC	12.1%	10.7%	699	1920	166
FUDS	27.7%	20.4%	74.0	610	−15.7

4.2. Estimation of diffusion coefficient D_s

4.2.1. Estimating D_s under constant model/sensor bias

In this case, we demonstrate the estimation of D_s subject to constant bias Δy in voltage. The procedures of data optimization, simulation data generation, and estimation are similar to those in Section 4.1.1, and

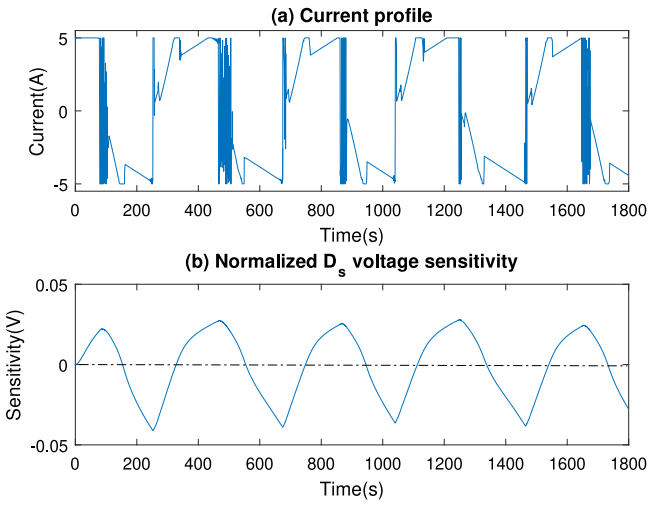

Fig. 3. Optimized current profile for estimating D_s subject to constant model/measurement bias using new approach.

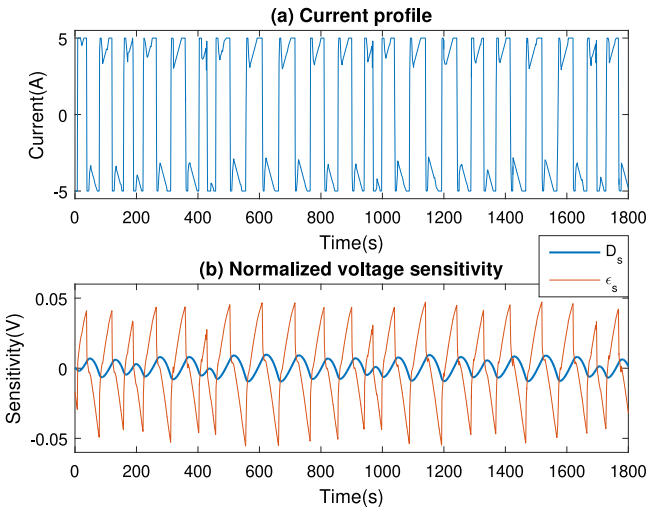

Fig. 4. Optimized current profile for estimating D_s subject to parameter uncertainty using new approach.

Table 3
Estimation results of D_s under constant bias in simulation.

Profile	Actual error	Predicted error	FI	$\sum_{k=1}^{N} \frac{\partial y_k}{\partial D_s}$
New approach	0.0550%	0.0629%	2.98	−0.0625
FI optimal	27.7%	23.2%	35.6	−382
Pulse	−128%	−139%	0.0600	1.22
1C CC	−44.3%	−60.5%	27.5	385
FUDS	−26688%	−11789%	0.0411	0.603

Table 4
Estimation results of D_s under parameter uncertainty in simulation.

Profile	Actual error	Predicted error	FI	$\sum_{k=1}^{N} \frac{\partial y_k}{\partial D_s} \cdot \frac{\partial y_k}{\partial \epsilon_s}$
New approach	6.62%	6.49%	0.119	−0.0747
FI optimal	−42.2%	−57.0%	22.8	82.4
Pulse	26.4%	22.9%	0.0249	−0.0697
1C CC	−54.9%	−81.3%	27.8	131
FUDS	−57.3%	−85.2%	1.57	7.67

hence not repeated. The input current profile optimized using the new approach is shown in Fig. 3. Estimation results using each profile are summarized in Table 3, which also shows the actual estimation error and predicted error calculated based on Eq. (10).

It is seen that the optimal current profile obtained based on the new approach significantly outperforms all other profiles, as it achieves the minimum error at 0.055%, which is much better than all others, with the closest one given by the traditional FI-based profile at 27.7%, which is 503 times as large. Similar to the case of ϵ_s, the dramatic improvement in accuracy can be explained by the evolution of sensitivity $\frac{\partial y_k}{\partial D_s}$ under the new profile, as shown in Fig. 3(b). Specifically, the profile obtained based on the new approach gives a near-zero $\sum_k^N \frac{\partial y_k}{\partial D_s} = -0.0625$, while the sensitivity under the FI-based profile is at $\sum_k^N \frac{\partial y_k}{\partial D_s} = -382$. Therefore, although the (Fisher) information level of the latter is higher, the estimation accuracy is still poor when subject to uncertainty. These results demonstrate the deficiency of the traditional FI-based approach, and the effectiveness of the new approach in rejecting uncertainty by incorporating $\sum_k^N \frac{\partial y_k}{\partial D_s} = 0$. On the other hand, the worst estimation result is given by the FUDS profile, whose error is more than 266 times the true D_s value. Even though the FUDS has a fairly small $\sum_k^N \frac{\partial y_k}{\partial D_s} = 0.603$, its small Fisher information (0.0411) leads to the poor estimation accuracy. These findings further emphasize the importance of considering both Fisher information and our newly identified data structures for data optimization.

Table 3 also shows that Eq. (10) can be effectively used for error quantification. For the proposed new optimal, FI-based optimal, CC and pulse profiles, the predicted estimation errors match well with the actual errors. The equation does not quite apply to the FUDS profile, mainly because the estimation result is too far off the actual value, and the derivation of Eq. (10) is based on first-order Taylor expansion around the estimate.

4.2.2. Estimating D_s under parameter uncertainty

In this case, D_s is estimated subject to parameter uncertainty in the electrode active material volume fraction ϵ_s. The procedures of data optimization, simulation data generation, and estimation are similar to those in Section 4.1.2, and hence not repeated. For estimation, the assumed value for ϵ_s was deviated by 10% from the true value (used in simulation for data generation) to emulate the parameter uncertainty. The optimization results using our proposed new method, i.e. solving Eq. (13) with $\alpha = 1$, are shown in Fig. 4.

Estimation results using each profile are summarized in Table 4, along with the actual and predicted errors calculated based on Eq. (10). It is seen that the profile optimized using the new approach achieves the minimum estimation error at 6.62%, which is better than all other profiles, with the FI-based approach at −42.2% and the pulse profile at 26.4% being the closest. The substantial improvement is attributed to the fact that the new profile is the only one designed to penalize $\left|\sum_k^N \frac{\partial y_k}{\partial D_s}\frac{\partial y_k}{\partial \epsilon_s}\right|$, i.e. accommodating orthogonal D_s and ϵ_s sensitivity, as shown in Table 4. It is also interesting to note from Fig. 4(b) that the sensitivity of the uncertain parameter ϵ_s is much higher than that of the target parameter D_s (by one order of magnitude). Traditionally, estimating weakly sensitive parameters under the shadow of uncertainty in strongly sensitive parameters is extremely difficult if not totally impossible, which is the reason why all other profiles yield significant estimation errors which are one order of magnitude higher. The explanation can be given by our derived error formula in Eq. (10). Specifically, the equation shows that the parameter uncertainty $\Delta\theta_2$ will propagate to the estimation error through $\sum_k^N \frac{\partial y_k}{\partial \theta_1}\frac{\partial y_k}{\partial \theta_2}\Delta\theta_2$. Therefore, high sensitivity of the uncertain parameter, i.e. $\frac{\partial y_k}{\partial \theta_2}$, will induce large estimation error. We show that by leveraging the orthogonal parameter sensitivity design, the weakly sensitive parameter can be estimated with satisfactory estimation accuracy.

5. Experimental validation

In this section, we present the experimental validation of the proposed new data optimization framework in the context of the battery electrochemical parameter estimation problem. Experiments have been performed using an Arbin LBT21084 cycler on a LGM50T INR21700 battery cell. Various current profiles, including the optimized profiles using the new and FI-based approaches and baseline profiles shown in Section 4, are applied as input excitation to generate the voltage data, which are then used for parameter estimation based on the least-squares algorithm and the SPMe model. The true parameter values for benchmarking the estimation error of the target variable and those of the remaining parameters are adopted from [37], which parameterized an LGM50 INR21700 battery with detailed electrochemical measurements. Some parameter values have been adjusted due to the slight difference in electrochemistry between the LGM50 and LGM50T batteries, e.g. the active material volume fraction. The results are shown for the estimation of the electrode active material volume fraction ε_s subject to different uncertainties under experimental conditions.

5.1. Estimating ε_s subject to model uncertainty

First, we consider the case of estimation subject to model/measurement uncertainty. Under experimental conditions, there is intrinsic model/measurement uncertainty with the estimation problem. Specifically, as no model could capture the system dynamics perfectly, there will always be mismatch between the actual and model-predicted output, even if all the parameters and measurements are accurate. In the context of the single particle battery model discussed in this paper, there are limiting assumptions, such as uniform current density and lithium concentration distribution across the electrode, which could lead to model imperfection [40,41]. In addition, model reduction procedures, e.g. Padé approximation used to simplify the original PDE-based diffusion equations, would also introduce mismatch between the model and true battery dynamics [19,42,43]. Such uncertainty could consist of a constant component, which is essentially the Δy term in Eq. (10), and a varying component, which can be represented by the δy_k term in Eq. (10). It is noted that the total model uncertainty is complicated as it changes over time and operating conditions. Therefore, model uncertainty will be different under different input profiles, which is difficult to know beforehand and hence design to compensate. Here we focus on demonstrating the effectiveness of the proposed data optimization approach in countering the constant component of the uncertainty. Specifically, the profile designed in Section 4.1.1 to minimize the error induced by the constant bias Δy is used to estimate ε_s and compare with the estimates given by other profiles.

The results are summarized in Table 5. It is seen that the proposed approach gives the best estimation accuracy with an actual error of −3.69%, whereas all other profiles yield at least twice as large of an error. Compared with the simulation results previously shown in Table 1, the error of the optimized profile is larger, mainly due to the varying component of the model uncertainty that has not been accommodated in data optimization. Nevertheless, the results still demonstrate the effectiveness of improving the estimation accuracy subject to model uncertainty by countering the constant component. In addition, we have also validated Eq. (10) for uncertainty quantification considering both constant and varying model uncertainty. Specifically, the differences between the measured battery voltage and the model prediction based on true parameter values are obtained for each profile, which are then applied to Eq. (10) as Δy and δy_k to compute the predicted estimation error. It can be seen that the predicted errors match well with the actual errors (which are computed as the difference between the estimated and true parameter values) for all profiles, validating the uncertainty propagation mechanisms established by our theoretic derivation.

Table 5
Estimation results of ε_s with model/measurement uncertainty in experiment.

Profile	ε_s Estimate	Actual error	Predicted error
New approach	0.582	−3.69%	−3.80%
FI optimal	0.610	−8.60%	−9.78%
Pulse	0.444	21.0%	14.0%
1C CC	0.645	−14.8%	−16.0%
FUDS	0.526	6.32%	5.42%

Table 6
Estimation results of ε_s with model/measurement and parameter uncertainty in experiment.

Profile	ε_s Estimate	Actual error	Predicted error
New approach	0.582	−3.69%	−5.52%
FI optimal	0.587	−4.52%	−5.87%
Pulse	0.442	21.4%	14.0%
1C CC	0.617	−9.94%	−11.3%
FUDS	0.508	9.62%	8.49%

5.2. Estimating ε_s subject to model and parameter uncertainty

In this case, we further consider parameter uncertainty in estimating ε_s under experimental conditions. The data optimization, experiment, and estimation procedures are mostly the same as in the previous case, except that the diffusion coefficient D_s is deviated by 20% in estimation to emulate parameter uncertainty. The profiles optimized based on the new and FI-based approaches are the same as in Section 4.1.2, as the former accommodates both the constant component of the model uncertainty and the parameter uncertainty in D_s. The results are summarized in Table 6, which show that the profile designed by the new approach outperforms all other profiles and the predicted errors match well with the actual errors. It is interesting to note that some profiles, especially the pulse and FUDS profiles, give better results than in simulation shown in Table 2. The reason is that the varying model uncertainty could cancel out some of the errors caused by other sources according to Eq. (10), if the signs of relevant terms are opposite. However, such cancellation is unpredictable in practice and cannot be expected/utilized. For example, if any of the error terms switch sign due to change in operating conditions, the total error will be significantly amplified.

6. Conclusion

In this paper, a new data analysis and optimization framework for dynamic system parameter estimation is formulated, which is capable of achieving excellent estimation accuracy subject to uncertainties in measurement, model, and parameters. Based on a newly derived equation for quantifying the errors of the least-squares parameter identification algorithm, we first identify several desirable data structures for rejecting uncertainties, beyond the traditional Fisher information criterion. For example, to counter constant measurement/model bias, it is desirable to have the sum of sensitivity of the target parameter equal to zero over the whole data sequence. Meanwhile, to counter parameter uncertainty, it is desirable to have the sensitivity vector of the target parameter orthogonal to that of the uncertain parameter. The new framework is then established by incorporating these data structures into the objective function (or constraints) of data optimization and leveraging the efficient sensitivity computation technique we developed previously. Finally, the framework is applied to the battery electrochemical parameter estimation problem in simulation and experiments subject to model and measurement uncertainties, and demonstrates superior uncertainty rejection capability over the traditional Fisher-information-based approach and other baselines. For example, by utilizing orthogonal sensitivity design, the new methodology enables accurate estimation of weakly sensitive parameters under the shadow of uncertainty in strongly sensitive parameters, which has

been traditionally considered as extremely difficult. Using the generated input profile for estimation reduces the estimation error by up to two orders of magnitude compared to the Fisher-information-based approach. Ongoing works include extension of the data optimization framework to multi-variable estimation and data selection/mining for online state/parameter estimation using real-time data stream.

CRediT authorship contribution statement

Qingzhi Lai: Methodology, Conceptualization, Software, Validation, Data curation, Writing - original draft. **Hyoung Jun Ahn:** Project administration, Funding acquisition, Conceptualization. **YoungJin Kim:** Validation. **You Na Kim:** Validation. **Xinfan Lin:** Conceptualization, Methodology, Supervision, Project administration, Funding acquisition, Writing - original draft, Resources.

Declaration of competing interest

The authors declare that they have no known competing financial interests or personal relationships that could have appeared to influence the work reported in this paper.

Acknowledgment

This work was supported by the LG Chem BIC program from LG Energy Solution Ltd., Seoul, Republic of Korea.

References

[1] Xiong R, Sun F, Chen Z, He H. A data-driven multi-scale extended Kalman filtering based parameter and state estimation approach of lithium-ion polymer battery in electric vehicles. Appl Energy 2014;113:463–76.
[2] Lin X, Kim Y, Mohan S, Siegel JB, Stefanopoulou AG. Modeling and estimation for advanced battery management. Annu Rev Control Robot Auton Syst 2019;2:393–426.
[3] Bi Y, Choe S-Y. An adaptive sigma-point Kalman filter with state equality constraints for online state-of-charge estimation of a Li (NiMnCo) O2/Carbon battery using a reduced-order electrochemical model. Appl Energy 2020;258:113925.
[4] Jiang LL, Maskell DL, Patra JC. Parameter estimation of solar cells and modules using an improved adaptive differential evolution algorithm. Appl Energy 2013;112:185–93.
[5] Chen K, Yu J. Short-term wind speed prediction using an unscented Kalman filter based state-space support vector regression approach. Appl Energy 2014;113:690–705.
[6] Wu FF. Power system state estimation: a survey. Int J Electr Power Energy Syst 1990;12(2):80–7.
[7] Al-Wakeel A, Wu J, Jenkins N. State estimation of medium voltage distribution networks using smart meter measurements. Appl Energy 2016;184:207–18.
[8] Lin X, Stefanopoulou A, Laskowsky P, Freudenberg J, Li Y, Anderson RD. State of charge estimation error due to parameter mismatch in a generalized explicit lithium ion battery model. In: ASME 2011 dynamic systems and control conference and bath/ASME symposium on fluid power and motion control. American Society of Mechanical Engineers Digital Collection; 2012, p. 393–400.
[9] Mendoza S, Liu J, Mishra P, Fathy H. On the relative contributions of bias and noise to lithium-ion battery state of charge estimation errors. J Energy Storage 2017;11:86–92.
[10] Lin X. Theoretical analysis of battery SOC estimation errors under sensor bias and variance. IEEE Trans Ind Electron 2018;65(9):7138–48.
[11] Zhang L, Lyu C, Hinds G, Wang L, Luo W, Zheng J, et al. Parameter sensitivity analysis of cylindrical LiFePO4 battery performance using multi-physics modeling. J Electrochem Soc 2014;161(5):A762.
[12] Perez HE, Moura SJ. Sensitivity-based interval PDE observer for battery SOC estimation. In: 2015 American control conference (ACC). IEEE; 2015, p. 323–8.
[13] Li W, Cao D, Jöst D, Ringbeck F, Kuipers M, Frie F, et al. Parameter sensitivity analysis of electrochemical model-based battery management systems for lithium-ion batteries. Appl Energy 2020;269:115104.
[14] Lin X, Stefanopoulou AG. Analytic bound on accuracy of battery state and parameter estimation. J Electrochem Soc 2015;162(9):A1879–91.
[15] Lin X. Analytic analysis of the data-dependent estimation accuracy of battery equivalent circuit dynamics. IEEE Control Syst Lett 2017;1(2):304–9.
[16] Sharma A, Fathy HK. Fisher identifiability analysis for a periodically-excited equivalent-circuit lithium-ion battery model. In: 2014 American control conference. IEEE; 2014, p. 274–80.
[17] Forman JC, Moura SJ, Stein JL, Fathy HK. Genetic identification and fisher identifiability analysis of the Doyle–Fuller–Newman model from experimental cycling of a LiFePO4 cell. J Power Sources 2012;210:263–75.
[18] Lai Q, Jangra S, Ahn HJ, Kim G, Joe WT, Lin X. Analytical sensitivity analysis for battery electrochemical parameters. In: 2019 American control conference (ACC). IEEE; 2019, p. 890–6.
[19] Lai Q, Jangra S, Ahn HJ, Kim G, Joe WT, Lin X. Analytical derivation and analysis of parameter sensitivity for battery electrochemical dynamics. J Power Sources 2020;472:228–338.
[20] Rothenberger MJ, Docimo DJ, Ghanaatpishe M, Fathy HK. Genetic optimization and experimental validation of a test cycle that maximizes parameter identifiability for a Li-ion equivalent-circuit battery model. J Energy Storage 2015;4:156–66.
[21] Park S, Kato D, Gima Z, Klein R, Moura S. Optimal experimental design for parameterization of an electrochemical lithium-ion battery model. J Electrochem Soc 2018;165(7):A1309–23.
[22] Song Z, Hofmann H, Lin X, Han X, Hou J. Parameter identification of lithium-ion battery pack for different applications based on Cramer-Rao bound analysis and experimental study. Appl Energy 2018;231:1307–18.
[23] Lai Q, Ahn HJ, Kim G, Joe WT, Lin X. Optimization of current excitation for identification of battery electrochemical parameters based on analytic sensitivity expression. In: 2020 American control conference (ACC). IEEE; 2020, p. 346–51.
[24] Cramér H. Mathematical methods of statistics, Vol. 9. Princeton university press; 1999.
[25] Lai Q, Kim G, Joe WT, Lin X. Data optimization for parameter estimation under system uncertainties with application to Li-ion battery. In: 2021 American control conference (ACC). IEEE; 2021, accepted.
[26] Scharf LL, McWhorter LT. Geometry of the Cramer-Rao bound. Signal Process 1993;31(3):301–11.
[27] Lin X. On the analytic accuracy of battery SOC, capacity and resistance estimation. In: 2016 American control conference (ACC). IEEE; 2016, p. 4006–11.
[28] Mishra PP, Garg M, Mendoza S, Liu J, Rahn CD, Fathy HK. How does model reduction affect lithium-ion battery state of charge estimation errors? Theory and experiments. J Electrochem Soc 2016;164(2):A237.
[29] Park S, Zhang D, Moura S. Hybrid electrochemical modeling with recurrent neural networks for li-ion batteries. In: 2017 American control conference (ACC). IEEE; 2017, p. 3777–82.
[30] Chen X, Dillen E, Fathy H, O'Connor J. Optimizing the design of a rijke tube experiment for combustion stability model identifiability. In: 2019 American control conference (ACC). IEEE; 2019, p. 4974–81.
[31] Schmidt AP, Bitzer M, Imre ÁW, Guzzella L. Experiment-driven electrochemical modeling and systematic parameterization for a lithium-ion battery cell. J Power Sources 2010;195(15):5071–80.
[32] Li J, Wang L, Lyu C, Wang H, Liu X. New method for parameter estimation of an electrochemical-thermal coupling model for LiCoO2 battery. J Power Sources 2016;307:220–30.
[33] Jin N, Danilov DL, Van den Hof PM, Donkers M. Parameter estimation of an electrochemistry-based lithium-ion battery model using a two-step procedure and a parameter sensitivity analysis. Int J Energy Res 2018;42(7):2417–30.
[34] Tian N, Wang Y, Chen J, Fang H. One-shot parameter identification of the Thevenin's model for batteries: Methods and validation. J Energy Storage 2020;29:101282.
[35] Tian N, Fang H, Chen J, Wang Y. Nonlinear double-capacitor model for rechargeable batteries: Modeling, identification, and validation. IEEE Trans Control Syst Technol 2020;29(1):370–84.
[36] Yuan S, Wu H, Ma X, Yin C. Stability analysis for li-ion battery model parameters and state of charge estimation by measurement uncertainty consideration. Energies 2015;8(8):7729–51.
[37] Chen C-H, Planella FB, O'Regan K, Gastol D, Widanage WD, Kendrick E. Development of experimental techniques for parameterization of multi-scale Lithium-ion battery models. J Electrochem Soc 2020;167(8):080534.
[38] Channagiri SA, Nagpure SC, Babu S, Noble GJ, Hart RT. Porosity and phase fraction evolution with aging in lithium iron phosphate battery cathodes. J Power Sources 2013;243:750–7.
[39] Fu R, Choe S-Y, Agubra V, Fergus J. Modeling of degradation effects considering side reactions for a pouch type Li-ion polymer battery with carbon anode. J Power Sources 2014;261:120–35.
[40] Di Domenico D, Stefanopoulou A, Fiengo G. Lithium-ion battery state of charge and critical surface charge estimation using an electrochemical model-based extended Kalman filter. J Dyn Syst Meas Control 2010;132(6):061302.
[41] Bartlett A, Marcicki J, Onori S, Rizzoni G, Yang XG, Miller T. Electrochemical model-based state of charge and capacity estimation for a composite electrode lithium-ion battery. IEEE Trans Control Syst Technol 2015;24(2):384–99.
[42] Marcicki J, Canova M, Conlisk AT, Rizzoni G. Design and parametrization analysis of a reduced-order electrochemical model of graphite/LiFePO4 cells for SOC/SOH estimation. J Power Sources 2013;237:310–24.
[43] Yang R, Xiong R, Shen W, Lin X. Extreme learning machine-based thermal model for lithium-ion batteries of electric vehicles under external short circuit. Engineering 2021;7(3):395–405.